Adaptive multiresolution semi-Lagrangian discontinuous Galerkin methods for the Vlasov equations

Nicolas Besse†

joint work with Eric Madaule and Erwan Deriaz

†Observatoire de la Côte d'Azur, Nice, France

Nicolas.Besse@oca.eu

Contents

1. Vlasov equations

2. Adaptive multiresolution Semi-Lagrangian discontinuous Galerkin methods

3. Numerical results

Vlasov equations

The Vlasov equation (plasma setting)

- $(x, \xi) \in \mathbb{R}^d \times \mathbb{R}^d$, $d = 1, ..., 3$: the phase-space
- $f(t, x, \xi)$: the statistical distribution function of particles
- Vlasovian regime: $(\nu_{coll}/\omega_p) \sim g = (n_0 \lambda_D^3)^{-1} \ll 1$:
  Individual and short-range interactions (collisions) are neglected.
  Collective and long-range Coulombian interactions are dominant and modelized by mean-fields:

$$\frac{\partial f}{\partial t} + v(\xi) \cdot \nabla_x f + (F_{\mathrm{self}}(t, x, \xi) + F_{\mathrm{applied}}(t, x, \xi)) \cdot \nabla_\xi f = 0$$

The relativistic velocity $v(\xi)$ is given by:

$$v(\xi) = \frac{\xi/m}{\sqrt{1 + |\xi|^2/(mc)^2}}.$$

$F_{\mathrm{self}}(t, x, \xi)$ is the Lorentz force given by:

$$F_{\mathrm{self}}(t, x, \xi) = q(E(t, x) + v(\xi) \times B(t, x)).$$

The charge and current density are given by the two first moments of f

$$\rho(t,x) = q\int_{\mathbb{R}^d} f(t,x,\xi)d\xi, \qquad j(t,x) = q\int_{\mathbb{R}^d} v(\xi)f(t,x,\xi)d\xi.$$

The Vlasov-Poisson system (VP) (plasma case):

$$B = 0, \quad E = -\nabla\phi, \quad -\Delta\phi = \rho/\varepsilon_0$$

The Vlasov-Quasistatic system (VQS):

$$E = -\nabla\phi, \quad -\Delta\phi = \rho/\varepsilon_0, \qquad B = \nabla\times A, \quad -\Delta A = \mu_0 j.$$

The Vlasov-Darwin system (VD):

$$\begin{cases} \dfrac{\partial E_{irr}}{\partial t} - c^2\nabla\times B = -\mu_0 c^2 j, \qquad \dfrac{\partial B}{\partial t} + \nabla\times E_{sol} = 0, \\[2ex] \nabla\cdot E_{irr} = \rho/\varepsilon_0, \quad \nabla\times E_{irr} = 0, \quad \nabla\cdot E_{sol} = 0, \quad \nabla B = 0, \\[2ex] E = E_{irr} + E_{sol} \end{cases}$$

The Vlasov-Maxwell system (VM):

$$\begin{cases} \dfrac{\partial E}{\partial t} - c^2\nabla \times B = -\mu_0 c^2 j, & \dfrac{\partial B}{\partial t} + \nabla \times E = 0, \\ \nabla \cdot E = \rho/\varepsilon_0, & \nabla \cdot B = 0. \end{cases}$$

For (VQS), (VD) and (VM) we have the compatibility condition for the source terms:

$$\frac{\partial \rho}{\partial t} + \nabla \cdot j = 0.$$

Other Vlasov systems:

- Vlasov-gravitational:
  Vlasov-Poisson, Vlasov-Nordström, Vlasov-Einstein, ...
- Vlasov-plasma, classic and quantum versions:
  Vlasov-waves, Vlasov-gyrokinetic,
  Vlasov-Wigner, Vlasov-Dirac-Benney, ...

Invariants

- $f_0(x,\xi) \geq 0 \Longrightarrow f(t,x,\xi) \geq 0,\ \forall t > 0$
- If f and β enough regular,

$$\int \beta(f(t,x,\xi))\, dxd\xi$$

- Especially the norm L^p, $1 \leq p \leq \infty$

  $L^\infty \Longrightarrow$ maximum principle
  $L^1 \Longrightarrow$ mass conservation
  $L^2 \Longrightarrow$ numerical dissipation

- $\beta(r) = r \ln r \Longrightarrow$ "Boltzmann" kinetic entropy conservation

$$H(t) = \int f(t,x,\xi) \ln f(t,x,\xi) dxd\xi.$$

- Energy conservation:

$$(\mathrm{VP}): \qquad \frac{1}{2m}\int f(t,x,\xi)|\xi|^2\, dxd\xi + \frac{\varepsilon_0}{2}\int |E(t,x)|^2\, dx,$$

(VM):

$$\int mc^2(\gamma(\xi)-1)f(t,x,\xi)|\xi|^2\, dxd\xi \; + \varepsilon_0 \int \frac{|E(t,x)|^2 + c^2|B(t,x)|^2}{2}\, dx$$

(VD):

$$\int mc^2(\gamma(\xi)-1)f(t,x,\xi)|\xi|^2\, dxd\xi \; + \varepsilon_0 \int \frac{|E_{irr}(t,x)|^2 + c^2|B(t,x)|^2}{2}\, dx$$

- momentum conservation:

  (VP):

$$\int f(t,x,\xi)\xi\, dxd\xi$$

  (VM):

$$\int f(t,x,\xi)\xi\, dxd\xi + \int \, dx\; \varepsilon_0 E(t,x)\times B(t,x)$$

  (VD):

$$\int f(t,x,\xi)\xi\, dxd\xi + \int \, dx\; \varepsilon_0 E_{irr}(t,x)\times B(t,x)$$

Characteristic curves equations

If $a(t, x, \xi) = (v(\xi), F(t, x, \xi))^T$ is enough regular (Lipschitz), we can introduce characteristic curves $(X(t; s, x, \xi), \Xi(t; s, x, \xi))$ associated to the first differential operator

$$\frac{\partial}{\partial t} + a.\nabla_{(x,\xi)}$$

which solves the classical ODEs equations

$$\begin{cases} \dfrac{dX}{dt}(t; s, x, \xi) = v(\Xi(t; s, x, \xi)), \\ \dfrac{d\Xi}{dt}(t; s, x, \xi) = F(t, X(t; s, x, \xi), \Xi(t; s, x, \xi)), \\ X(s; s, x, \xi) = x, \ \ \Xi(s; s, x, \xi) = \xi, \end{cases}$$

In the case of (VP), (VQS), (VD) and (VM), as

$$\nabla_{(x,\xi)} \cdot a = 0$$

the jacobian of the map

$$(x,\xi) \mapsto (X,\Xi) = \varphi_t(x,\xi) = (X(t;s,x,\xi),\Xi(t;s,x,\xi)),$$

remains constant and the Lagrangian flow $\varphi_t(x,\xi)$ preserves the measure and the connexity of the phase-space volume during time (phase-space incompressibility). This property implies the equivalence between the advective and the conservation form of the Vlasov Eq.:

$$\partial_t f + a \cdot \nabla_{(x,\xi)} f = 0 \quad \Longleftrightarrow \quad \partial_t f + \nabla_{(x,\xi)} \cdot (af) = 0,$$

which traduces conservation of the matter (continuity equation in phase-space). The advective form traduces the fact that f is constant along characteristic curves

$$f(t,x,\xi) = f(s,X(s;t,x,\xi),\Xi(s;t,x,\xi)).$$

RK: When variables are non-canonical φ_t is no more a volume-preserving map; the defect is compensated by the jacobian of the map "canonical $\leftrightarrow$non-canonical", but the flow is intrinsically volume-preserving (Liouville Th.)

Adaptive multiresolution Semi-Lagrangian discontinuous Galerkin methods

The principle of discontinuous-Galerkin method

0) We consider a 1D scalar conservation law, because the multi-dimensional case is solved by using splitting methods.

1) 1D scalar conservation law, $f = f(t,x)$,

$$\partial_t f + \partial_x (a(t,x) f) = 0 \quad + \text{initial conditions} + \text{boundary conditions}$$

2) We multiply the equation by a test fonction $\varphi \in V$, and we integrate on *each* cell I_i

$$\int_{I_i} (\partial_t f + \partial_x (af))\, \varphi \, dx = 0, \quad \forall \varphi \in V.$$

3) Weak formulation in space of the equation: integration by parts (IBP).

$$\int_{I_i} (\partial_t f \varphi - af \partial_x \varphi)\ dx + \int_{\partial I_i} af \cdot n \varphi \, d\gamma = 0, \quad \forall \varphi \in V.$$

4) Since V is a space of discontinuous functions, we replace fluxes by “numerical fluxes” at cell interfaces

$$\int_{I_i} (\partial_t f \varphi - af \partial_x \varphi)\ dx - (\widehat{af}\varphi)_{i-1/2} + (\widehat{af}\varphi)_{i+1/2} = 0, \quad \forall \varphi \in V$$

5) The choice of V (polynomial basis which can differ from a cell to another one) and numerical fluxes determine the properties of the numerical scheme (stability, consistency, convergence, high-order accuracy, conservation)

The semi-Lagrangian discontinuous Galerkin method (SLDG)*

After time integration between t^n and t^{n+1} we get, with $f_h(t,x) = S_t(f_h^n)$ (where $S_t(f_h^n)$ is the exact evolution operator starting with the initial condition f_h^n),

$$\int_{I_i} f_h^{n+1} \cdot \varphi \, dx = \int_{I_i} f_h^n \cdot \varphi \, dx + \int_{t^n}^{t^{n+1}} \int_{I_i} a(t,x) S_t(f_h^n) \cdot \partial_x \varphi \, dx \, dt$$
$$- \int_{t^n}^{t^{n+1}} \left(a(t,x) S_t(f_h^n) \cdot \varphi|_{x_{i+1/2}^-} - a(t,x) S_t(f_h^n) \cdot \varphi|_{x_{i-1/2}^+} \right) dt.$$

A space-time integration by parts (Divergence theorem) of the conservation law on the domain $\Omega_{i-1/2}$ (cf. figure), transforms the time integration between t^n and t^{n+1} into a space integration (at time t^n) which uses origin of characteristic curves at time t^n (noted x^*).
This integral is evaluated by using a Gauss-Legendre quadrature formula:

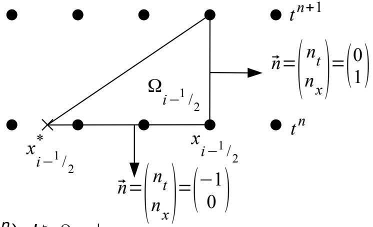

$$\int_{I_i} f_h^{n+1} \cdot \varphi \, dx = \int_{I_i} f_h^n \cdot \varphi \, dx + \Delta x_i \sum_{i_g} w_{i_g} \int_{\tilde{x}^*_{i_g}}^{\tilde{x}_{i_g}} f_h(\xi, t^n) \, d\xi \cdot \partial_x \varphi|_{\tilde{x}_{i_g}}$$
$$- \int_{x^*_{i+1/2}}^{x_{i+1/2}} f_h(\xi, t^n) \, d\xi \cdot \varphi(x^-_{i+1/2}) + \int_{x^*_{i-1/2}}^{x_{i-1/2}} f_h(\xi, t^n) \, d\xi \cdot \varphi(x^+_{i-1/2})$$

*Qiu-Shu JCP 11

The characteristic discontinuous Galerkin method (CDG)*

- Principle: we solve a dual problem. Indeed a test function $\varphi(x) \in V$ (taken as final condition at time t^{n+1}) is advected backward to the time t^n by the advection field $a(t,x)$. We then get:

$$\int_{I_i} f_h^{n+1}(x)\varphi(x)\,dx = \int_{I_i^*} f_h(t^n,x)\varphi(t^n,x)\,dx, \quad I_i^* = [x^*_{i-1/2}, x^*_{i+1/2}]$$

$$\approx \sum_{\ell}\sum_{i_g} w_{i_g} f_h(x^*_{i,\ell,i_g}, t^n)\varphi(x_{i,\ell,i_g})\Gamma(I^*_{i,\ell})$$

  - $x^*_{i\pm1/2}$: origin of characteristics at time t^n, coming from mesh points $x_{i\pm1/2}$ at t^{n+1}.
  - Index " ℓ " labels intersected cells.
  - Index " i_g " labels quadrature points (Gauss-Legendre).
  - $\Gamma(I^*_{i,\ell})$ is the measure of the intersection between cells I_i^* and I_ℓ.
- The method is illustrated by the following figure:

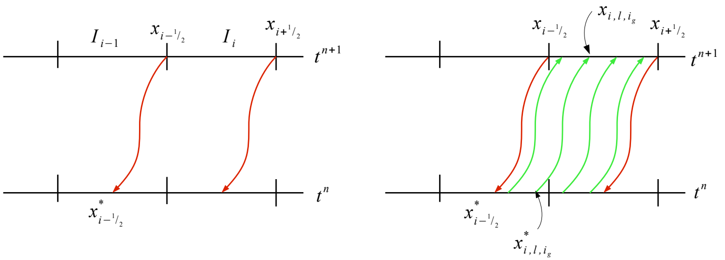

*Guo-Nair-Qiu MWR 14

Principle of AMR

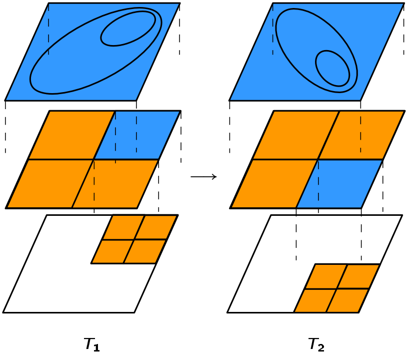

Example adaptive.

Black: level lines of the distribution function and mesh.

Blue: inactive cells, created but not used for computation.

Orange: active cells, created and used for computation.

Here, we see that 3 levels are created, two of which are used for computation.

The mesh is more refined where variations of level lines are important.

The typical loop of the algorithm:

- We suppose that we have an initial multi-wavelet representation of the distribution function associated to an initial (adaptive) mesh.
- Predict a new adaptive mesh by advecting forward (with a low-order scheme) cells of the initial mesh: Apply cell creation & cell refinement.
- Apply SLDG or CDG schemes by using the initial multi-wavelet representation of the distribution function projected on the predicted mesh. We then get a new multi-scale distribution function.
- Use a multi-wavelet decomposition of the new distribution function to discard details smaller than prescribed threshold: coarsening.

An example of adaptive mesh prediction

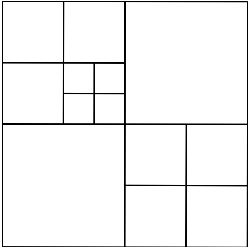

Initial mesh M^n.

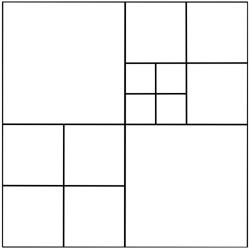

Predicted mesh after forward advection.

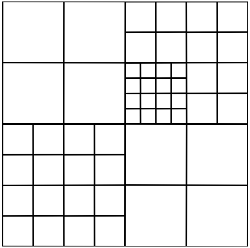

Predicted mesh after refinement.

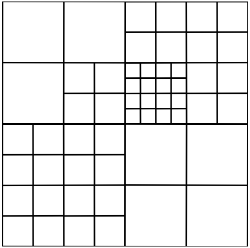

Merged mesh M^{n+1}.

Multi-scale representation by means of multi-wavelets basis

- We consider the spaces V_n^k of $\text{Dim}(V_n^k) = 2^n(k+1)$ and defined by

$$V_n^k = \{f:\ f|_{[2^{-n}l, 2^{-n}(l+1)]} \in \mathbb{P}^k,\ l = 0, \ldots 2^n - 1,\ f \text{ elsewhere}\},\ k \in \mathbb{N},\ n \in \mathbb{N}.$$

- We have inclusions

$$V_0^k \subset V_1^k \subset \cdots \subset V_n^k \subset \cdots \subset L^2.$$

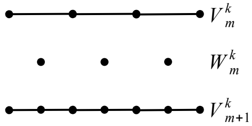

- The multi-wavelets space W_n^k is defined such that

$$V_{n+1}^k = V_n^k \oplus W_n^k \quad \text{and} \quad V_n^k \perp W_n^k.$$

- We then have the multi-scale decomposition:

$$V_n^k = V_0^k \oplus W_0^k \oplus W_1^k \oplus \ldots \oplus W_{n-1}^k,$$

or in other words the multi-scale representation of f:

$$f(t,x) = \sum_{j=0}^{k-1} \left(s_{j,0}^0(t)\phi_j(x) + \sum_{m=0}^{n-1} \sum_{l=0}^{2^m-1} d_{j,l}^m(t)\psi_{j,l}^m(x) \right)$$

- If $\{\phi_j\}_{j=0..k-1}$ is a basis for V_0^k then $\phi_{j,l}^n(x) = 2^{n/2}\phi_j(2^n x - l)$ is a basis for V_n^k.
  If $\{\psi_j\}_{j=0..k-1}$ is a basis for W_0^k then $\psi_{j,l}^n(x) = 2^{n/2}\psi_j(2^n x - l)$ is a basis for W_n^k.
- $s_{j,0}^0$: scale coefficient. $d_{j,l}^k$: wavelet coefficient.
- Threshold criterion: if $\|d_{\cdot,l}^m\|_{\ell^2} < \epsilon_m(\epsilon_0, m)$, then ignore details of level $\geq m$

Numerical results*

* Besse-Deriaz-Madaule JCP 332 2017

Error for linear transport: rotation

threshold	$\langle h \rangle$	L^1 error	L^1 order	L^2 error	L^2 order	L^∞ error	L^∞ order
0.1	4.47	2.57	-	0.401	-	0.210	-
0.01	2.09	0.0523	5.10	0.0149	4.32	0.0173	3.27
0.001	1.14	5.98 E -3	4.43	1.39 E -3	4.14	1.52 E -3	3.60
1 E -4	0.529	6.31 E -4	3.89	1.46 E -4	3.71	2.94 E -4	3.08
1 E -5	0.236	6.53 E -5	3.60	1.42 E -5	3.48	2.84 E -5	3.03

Error obtained with the AMW-SLDG scheme for polynomials of degree 2.

threshold	$\langle h \rangle$	L^1 error	L^1 order	L^2 error	L^2 order	L^∞ error	L^∞ order
0.1	4.47	0.786	-	0.179	-	0.357	-
0.01	2.43	0.0118	6.87	3.72 E -3	6.33	6.81 E -3	6.47
0.001	2.09	5.85 E -3	6.42	1.34 E -3	6.42	1.72 E -3	6.99
1 E -4	1.23	1.38 E -3	4.92	3.03 E -4	4.95	4.63 E -4	5.16
1 E -5	0.625	7.11 E -5	4.73	1.76 E -5	4.69	4.22 E -5	4.59

Error obtained with the AMW-SLDG scheme for polynomials of degree 3.

threshold	$\langle h \rangle$	L^1 error	L^1 order	L^2 error	L^2 order	L^∞ error	L^∞ order
0.1	4.47	2.57	-	0.401	-	0.210	-
0.01	2.09	0.0538	5.07	0.0149	4.31	0.0184	3.19
0.001	1.14	7.87 E -3	4.23	1.77 E -3	3.97	1.67 E -3	3.54
1 E -4	0.527	6.90 E -4	3.85	1.45 E -4	3.71	2.81 E -4	3.09
1 E -5	0.236	1.31 E -4	3.36	2.36 E -5	3.31	2.84 E -5	3.03

Error obtained with the AMW-CDG scheme for polynomials of degree 2.

threshold	$\langle h \rangle$	L^1 error	L^1 order	L^2 error	L^2 order	L^∞ error	L^∞ order
0.1	4.47	0.787	-	0.179	-	0.357	-
0.01	2.43	0.0118	6.87	3.72 E -3	6.33	6.81 E -3	6.47
0.001	2.09	5.88 E -3	6.42	1.34 E -3	6.42	1.72 E -3	6.99
1 E -4	1.24	1.45 E -3	4.90	3.08 E -4	4.95	4.63 E -4	5.17
1 E -5	0.626	1.18 E -4	4.47	2.71 E -5	4.49	5.57 E -5	4.46

Error obtained with the AMW-CDG scheme for polynomials of degree 3.

Error for nonlinear transport: Burgers equation

threshold	$\langle h \rangle$	L^1 error	L^1 order	L^2 error	L^2 order	L^∞ error	L^∞ order
0.1	1.25	0.204	-	0.0860	-	0.0839	-
0.01	0.313	0.0105	2.14	3.80 E -3	2.25	3.54 E -3	2.28
0.001	0.157	1.30 E -3	2.43	4.78 E -4	2.50	4.65 E -4	2.50
1 E -4	0.0869	2.49 E -4	2.51	9.00 E -5	2.57	1.34 E -4	2.41
1 E -5	0.0412	2.40 E -5	2.65	8.28 E -6	2.71	1.00 E -5	2.64

Error obtained with the AMW-SLDG scheme for polynomials of degree 2.

threshold	$\langle h \rangle$	L^1 error	L^1 order	L^2 error	L^2 order	L^∞ error	L^∞ order
0.1	1.25	0.187	-	0.0612	-	0.0454	-
0.01	0.627	8.94 E -3	4.38	2.99 E -3	4.36	2.88 E -3	3.98
0.001	0.313	5.26 E -4	4.24	1.89 E -4	4.17	2.09 E -4	3.88
1 E -4	0.198	1.78 E -4	3.77	7.46 E -5	3.64	1.09 E -4	3.27
1 E -5	0.157	3.28 E -5	4.16	1.19 E -5	4.11	1.38 E -5	3.89

Error obtained with the AMW-SLDG scheme for polynomials of degree 3.

threshold	$\langle h \rangle$	L^1 error	L^1 order	L^2 error	L^2 order	L^∞ error	L^∞ order
0.1	1.25	0.204	-	0.0860	-	0.0839	-
0.01	0.313	0.0105	2.14	3.80 E -3	2.25	3.54 E -3	2.28
0.001	0.157	1.30 E -3	2.43	4.78 E -4	2.50	4.65 E -4	2.50
1 E -4	0.0869	2.48 E -4	2.52	9.00 E -5	2.57	1.34 E -4	2.41
1 E -5	0.0412	2.30 E -5	2.66	8.16 E -6	2.71	1.03 E -5	2.64

Error obtained with the AMW-CDG scheme for polynomials of degree 2.

threshold	$\langle h \rangle$	L^1 error	L^1 order	L^2 error	L^2 order	L^∞ error	L^∞ order
0.1	1.25	0.187	-	0.0612	-	0.0454	-
0.01	0.627	8.94 E -3	4.38	2.99 E -3	4.36	2.88 E -3	3.98
0.001	0.313	5.26 E -4	4.24	1.89 E -4	4.17	2.08 E -4	3.88
1 E -4	0.198	1.78 E -4	3.77	7.46 E -5	3.64	1.08 E -4	3.27
1 E -5	0.157	3.24 E -5	4.16	1.19 E -5	4.11	1.34 E -5	3.91

Error obtained with the AMW-CDG scheme for polynomials of degree 3.

Plasma case: bump-on-tail 1/2

I.C.: $$f_0(x,v) = \frac{(1+0.04\cos(0.5x))}{10\sqrt{2\pi}}\left(9\exp\left(\frac{-v^2}{2}\right) + 2\exp\left(-2(v-4.5)^2\right)\right), \quad (x,v) \in [0, 20\pi] \times [-9, 9].$$

$\Delta t = 0.1$. Maximum level of refinement is 8. Polynomial degree is 2. Threshold $\epsilon_0 = 3 \times 10^{-3}$.

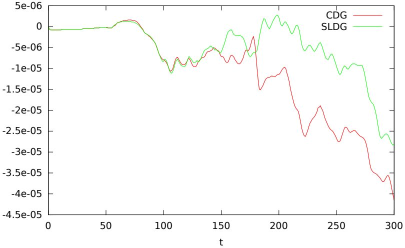

Relative variation of mass.

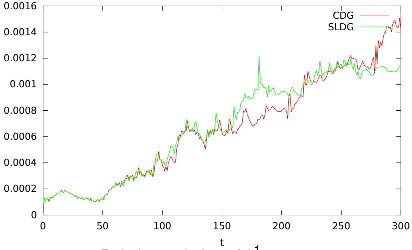

Relative variation of L^1-norm.

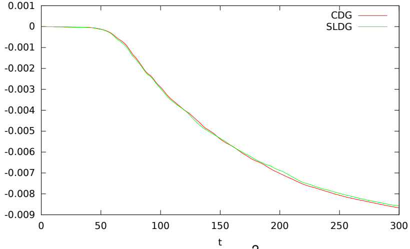

Relative variation of L^2-norm.

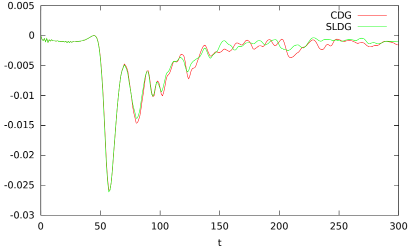

Relative variation of total energy.

Plasma case: bump-on-tail 2/2

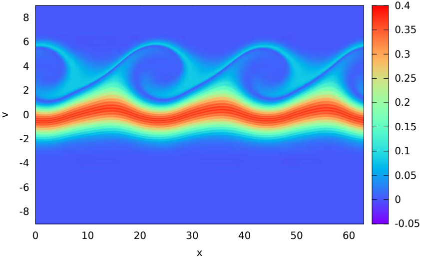

Distribution function at $t = 60$ pp.

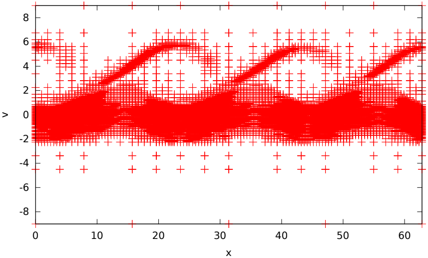

Mesh at $t = 60$ pp.

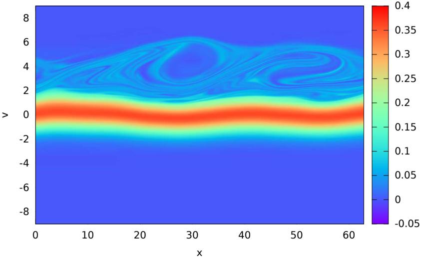

Distribution function at $t = 200$ pp.

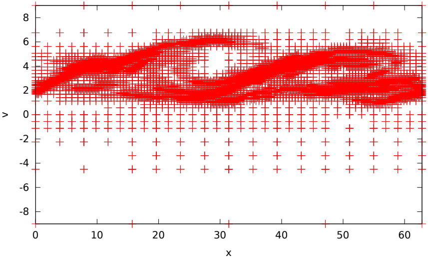

Mesh at $t = 200$ pp.

Distribution function and Mesh for bump on tail with the AMW-SLDG scheme.

Plasma case: focusing beam 1/2

Vlasov-Poisson equation with cylindrical symmetry:

$$\partial_t f(r,v,t) + \partial_r \left(\frac{v}{\varepsilon} f(r,v,t) \right) + \partial_v \Big(\left(E_\varepsilon(r,t) + F_\varepsilon(r,t)\right) f(r,v,t) \Big) = 0,$$

$$\frac{1}{r}\partial_r(rE_\varepsilon(r,t)) = \rho(r,t).$$

Initial Condition: $f_0(r,v) = \dfrac{3}{4v_{th}} \exp\left(\dfrac{-v^2}{2v_{th}^2}\right) \mathbb{1}_{[-1.8,1.8]}(r), \quad (r,v) \in [-3,3]^2.$

Focusing external field: $F_\varepsilon(r,t) = r\left(\dfrac{-1}{\varepsilon} + \cos^2\left(\dfrac{t}{\varepsilon}\right)\right).$

$\varepsilon = 0.1$. $v_{th} = 0.07$. $\Delta t = 0.02$. Polynomials of degree up to 2.

Maximum level of refinement is 8. Threshold $\epsilon_0 = 10^{-2}$.

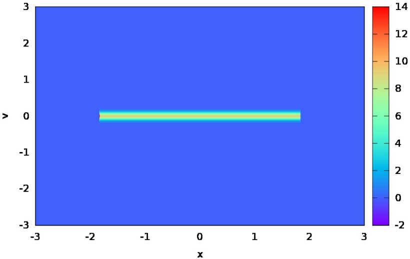

Initial distribution function.

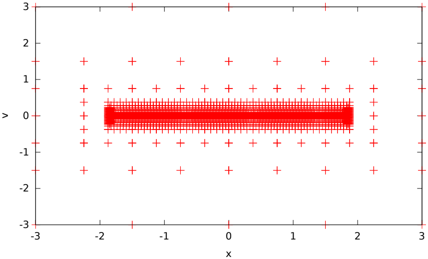

Initial mesh.

Plasma case: focusing beam 2/2

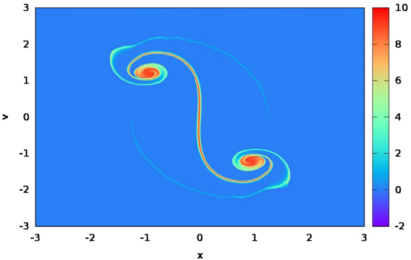

Distribution function at $t = 16$.

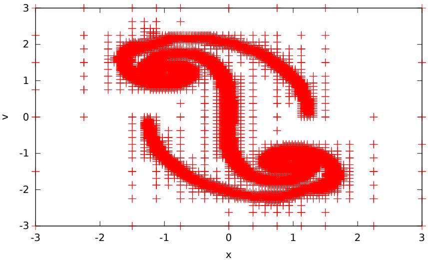

Mesh at $t = 16$.

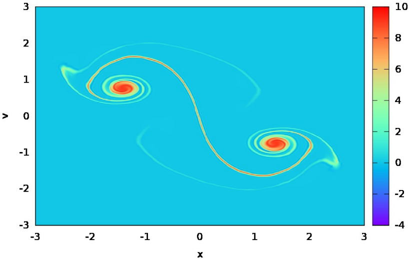

Distribution function at $t = 20$.

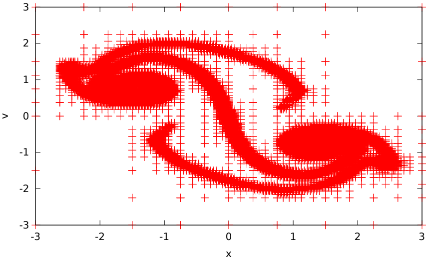

Mesh at $t = 20$.

Distribution function and mesh for focusing beam with the AMW-SLDG scheme.

Astrophysic case: cold layer 1/2

$$f_0(x,v) = \frac{1}{0.15\sqrt{2\pi}} \exp\left(-\frac{(v-u(x))^2}{2\times 0.15^2}\right), \quad (x,v)\in[0,2\pi]\times[-10,10],$$

$$u(x) = 0.01\sin(x).$$

$\Delta t = 0.02$.
Polynomials of degree 2.
Maximum level of refinement is 8.
Threshold is $\epsilon_0 = 3\times 10^{-3}$.

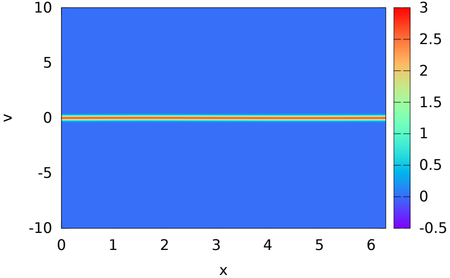

Initial distribution function.

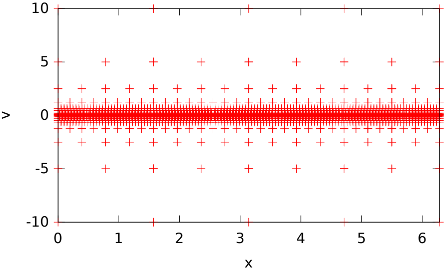

Initial mesh.

Astrophysic case: cold layer 2/2

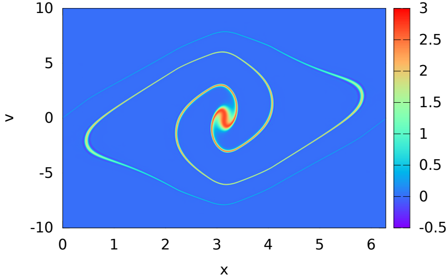

AMW-CDG

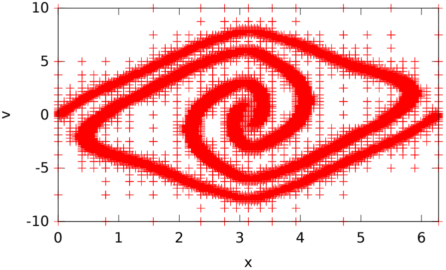

AMW-CDG

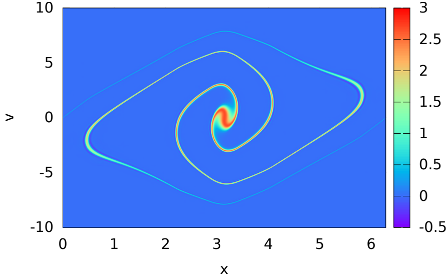

AMW-SLDG

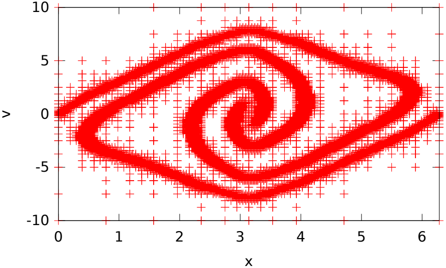

AMW-SLDG

Distribution function and mesh at $t = 3$.

Astrophysic case: gaussian distribution 1/3

$$\text{Initial condition: } f_0(x,v) = 4\exp\left(-\frac{(x^2+v^2)}{0.08}\right), \quad (x,v)\in[-2,2]^2$$

$\Delta t = 0.1$. Polynomials of degree up to 3. Maximum level of refinement is 9. Threshold is $\epsilon_0 = 3 \times 10^{-3}$.

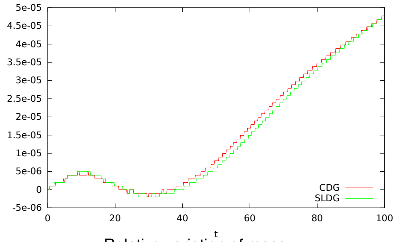

Relative variation of mass.

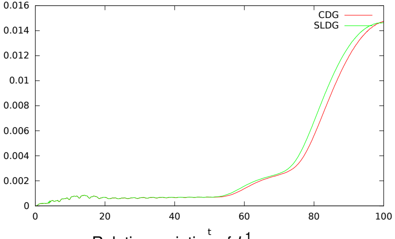

Relative variation of L^1-norm.

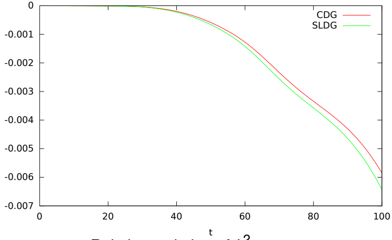

Relative variation of L^2-norm.

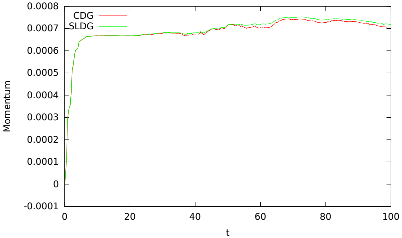

Variation of momentum.

Astrophysic case: gaussian distribution 2/3

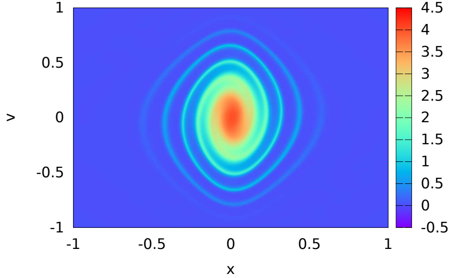

AMW-CDG

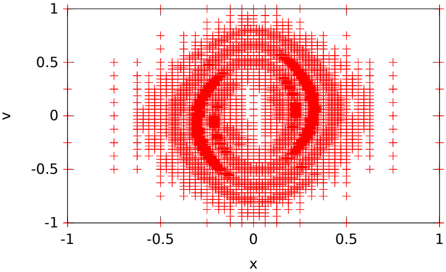

AMW-CDG

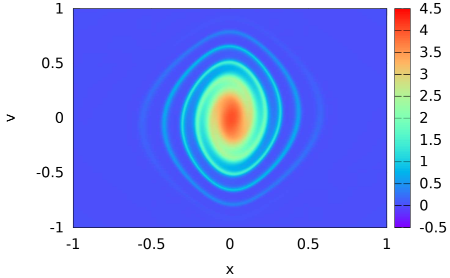

AMW-SLDG

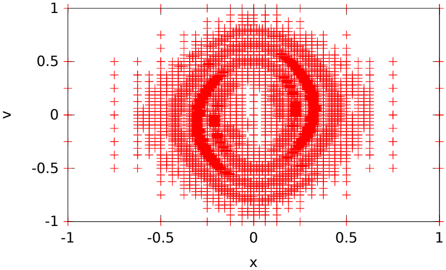

AMW-SLDG

Distribution function and mesh at $t = 15$.

Astrophysic case: gaussian distribution 3/3

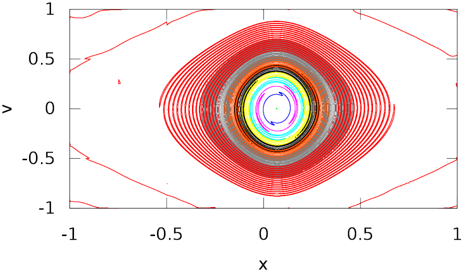

AMW-CDG

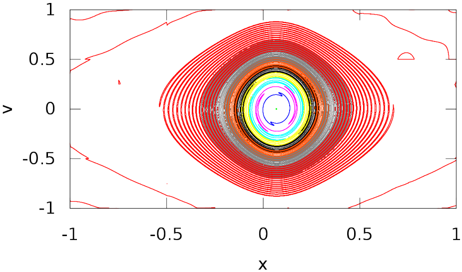

AMW-SLDG

Level lines of the distribution function at $t = 100$.

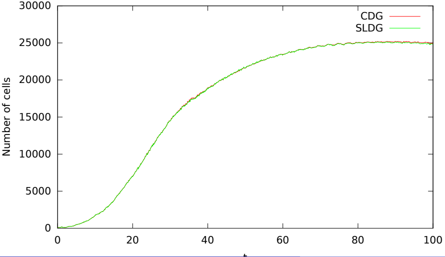

◀ Number of cells

- Adaptive mesh: 25000 cells
- Uniform mesh on $[-2, 2]^2$: 262000 cells
- Uniform mesh on $[-1, 1]^2$: 65500 cells

Astrophysic case: Jeans instability and return to BGK stationary state

$$f(x,v,0) = \frac{\exp\left(\frac{-v^2}{2}\right)}{\sqrt{2\pi}}(1 - A\cos(kx)), \quad (x,v) \in [0, 2\pi/k] \times [-V_c, V_c].$$

$A = 0.01, \quad k = 0.8 \quad$ and $\quad V_c = 6. \quad \Delta t = 0.1.$
Polynomials of degree 2.
Maximum level of refinement is 8.

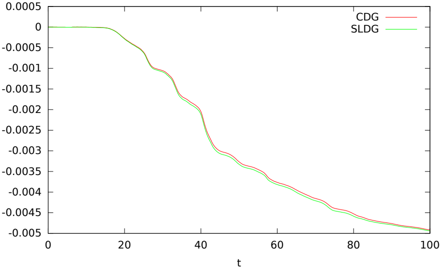

$\epsilon_0 = 0.003, \quad$ 8 refinement levels

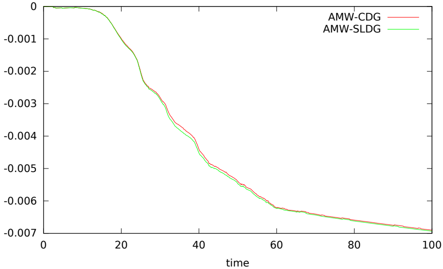

$\epsilon_0 = 0.01, \quad$ 7 refinement levels

Time evolution of L^2-norm

Astrophysic case: Jeans instability and return to BGK stationary state

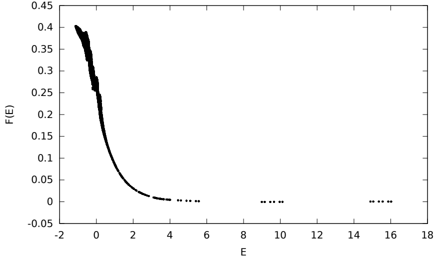

$E = v^2/2 - \phi(t = 100, x)$, $\epsilon_0 = 0.003$, 8 refinement levels

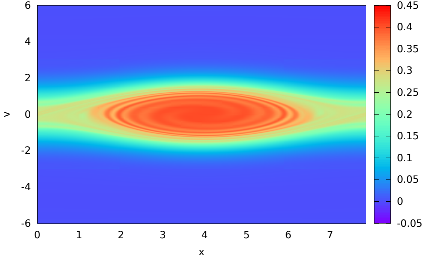

$f(t = 100, x, v)$, $\epsilon_0 = 0.003$, 8 refinement levels

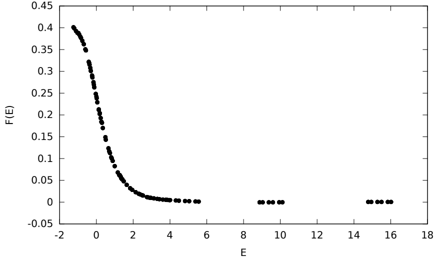

$E = v^2/2 - \phi(t = 100, x)$, $\epsilon_0 = 0.01$, 7 refinement levels

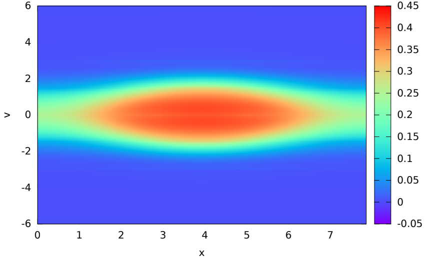

$f(t = 100, x, v)$, $\epsilon_0 = 0.01$, 7 refinement levels

AMW-CDG scheme

THANK YOU FOR YOUR ATTENTION